J Prev Alz Dis 2022;3(9):499-506
Published online February 7, 2022, http://dx.doi.org/10.14283/jpad.2022.24

Original Research



# Decreased Gray–White Matter Contrast of [11C]-PiB Uptake in Cognitively Unimpaired Subjects with Severe Obstructive Sleep Apnea

*S. Ylä-Herttuala[1,2], M. Hakulinen[3,4], P. Poutiainen[5], J. Lötjönen[6], M. Könönen[1,4,7], H. Gröhn[3], R. Vanninen[7,8], H. Mussalo[3], T. Laitinen[3,9], E. Mervaala[1,2]*

1. Dept. of Clinical Neurophysiology, Kuopio University Hospital, Finland; 2. Dept. of Clinical Neurophysiology, University of Eastern Finland, Kuopio, Finland; 3. Dept. of Clinical Physiology and Nuclear Medicine, Kuopio University Hospital, Finland; 4. Dept. of Applied Physics, University of Eastern Finland, Kuopio, Finland; 5. Dept. of Cyclotron and Radiopharmacy, Kuopio University Hospital, Finland; 6. Combinostics Ltd, Tampere, Finland; 7. Dept. of Radiology, Kuopio University Hospital, Finland; 8. Dept. of Radiology, University of Eastern Finland, Kuopio, Finland; 9. Dept. of Clinical Physiology and Nuclear Medicine, University of Eastern Finland, Kuopio, Finland

*Corresponding Author*: Professor Esa Mervaala, M.D., Ph.D. Department of Clinical Neurophysiology, Kuopio University Hospital, POB 100, 70029 KYS, Finland, ORCID ID: 0000-0001-5682-5747, Mobile: +358-44-7113245, Email: esa.mervaala@kuh.fi, Fax: +358-17-173244

## Abstract

BACKGROUND: Very recently, cognitively normal, middle-aged adults with severe obstructive sleep apnea (OSA) were shown to have regional cortical amyloid-β deposits. In the normal brain, amyloid tracer (e.g., [11C]-PiB) uptake is observed in white matter (WM) but not in cortical gray matter (GM), resulting in clear GM–WM contrast. There are no reports on possible changes in this contrast in severe OSA.

OBJECTIVES: Evaluate changes in the global [11C]-PiB GM–WM contrast and study if factors reflecting clinical and imaging characteristics are associated with them.

DESIGN AND SETTING: Cross-sectional imaging study.

PARTICIPANTS: 19 cognitively intact middle-aged (mean 44 years) patients with severe OSA (Apnea–Hypopnea Index >30/h), carefully selected to exclude any other possible factors that could alter brain health.

MEASUREMENTS: Detailed neuroimaging (amyloid PET, MRI). Signs of possible alterations in amyloid tracer GM–WM contrast and kinetics were studied with static and dynamic [11C]-PiB PET and WM structures with detailed 3.0T MRI.

RESULTS: Static [11C]-PiB PET uptake showed significantly decreased GM–WM contrast in 5 out of 19 patients. This was already clearly seen in visual evaluation and also detected quantitatively using retention indexes. Dynamic imaging revealed decreased contrast due to alterations in trace accumulation in the late phase of [11C]-PiB kinetics. Decreased GM–WM contrast in the late phase was global in nature. MRI revealed no corresponding alterations in WM structures. Importantly, decreased GM–WM contrast was associated with smoking ($p = 0.007$) and higher Apnea–Hypopnea Index ($p = 0.001$).

CONCLUSIONS: Severe OSA was associated with decreased GM–WM contrast in amyloid tracer uptake, with significant correlation with clinical parameters of smoking and AHI. The results support and further extend the current understanding of the deleterious effect of severe OSA on proper amyloid clearance, possibly reflecting dysfunction of the brain glymphatic system.

*Key words: Amyloid, PET, sleep apnea, Alzheimer's disease.*

## Introduction

The most common and prevalent sleep disorder, obstructive sleep apnea (OSA), has been linked to the possible risk for Alzheimer's disease (AD), mostly due to findings of brain amyloid-β (Aβ) burden in OSA patients. Recently, cortical Aβ deposits in positron emission tomography (PET) studies have been described in unimpaired older adults with OSA (mean age 69 years) (1). Importantly, younger patients (mean age 57 years) with severe OSA have also shown evidence of brain amyloid burden (2). Furthermore, we recently reported similar findings in middle-aged (mean age 44 years), cognitive intact patients with severe OSA (3). These studies have described typically cortical amyloid deposits. ln amyloid PET-imaging using [11C]-Pittsburg compound B (PiB), white matter (WM) should display a significant amount of amyloid tracer uptake, and no cortical gray matter (GM) accumulation should occur, resulting in clear and visually detectable GM–WM contrast in the normal brain.

Structural changes in WM integrity have been shown in several magnetic resonance imaging (MRI) studies in OSA (4, 5), suggesting at least WM changes (6), or even WM injury (7, 8), in some OSA patient populations. Amyloid imaging using [11C]-PiB has been suggested to reflect WM integrity (9, 10). Several studies have described an association between WM hyperintensities/lesions (WMH/WML) and reduced WM PiB uptake (11-14). It has been suggested that WML are linked to enhanced Aβ accumulation (15), and this amyloid burden might mediate age-related, cognitive differences (16).

Studying the GM–WM contrast necessitates exploration of possible alterations both in GM and WM. Important evidence on the dynamics of Aβ burden progression in GM areas shows a regional and sequential appearance (17, 18). An issue not explored before is the possible alterations between GM and WM uptake contrast. No data exist on whether this contrast

*Received November 19, 2021*
*Accepted for publication December 29, 2021*

would be changed without any structural evidence of WM alterations. In unimpaired elderly subjects, the earliest accumulation of Aβ fibrils may be associated with increased functional connectivity, and this may occur before structural alterations in MRI are present (19).

We studied GM–WM PiB uptake contrast in a carefully selected, middle-aged cohort of patients with severe OSA. Our objectives were to evaluate changes in the global [11C]-PiB GM–WM contrast and study if factors reflecting clinical and imaging characteristics are associated with it.

## Methods

### *Patients*

The cohort population was collected retrospectively from a routine diagnostic patient population that was evaluated at Kuopio University Hospital due to clinical suspicion of OSA. It consisted of 19 middle-aged patients (5 females) with findings of severe OSA in their diagnostic respiratory polygraphy. Home sleep apnea testing (HSAT) evaluations were conducted using an Embletta polygraphic device (Natus Medical Inc., CA, USA) and RemLogic version 3.2 software (Embla Systems LCC, Broomfield, CO, USA). The respiratory polygraphic OSA diagnosis was based on routinely used American Association of Sleep Medicine guidelines (20). Initially, the medical records of all patients studied between 2011 and 2018 were reviewed, from which eligible patients were carefully selected to complete the aims of the study. Several inclusion criteria were used: 1) age 30–50 years; 2) no medical history of major neurological diseases; 3) no history of psychiatric illness; 4) diabetes, when present, had to be in good treatment balance; 5) no use of medication influencing the central nervous system or any substance abuse; 6) no subjective or objective symptoms or signs of cognitive difficulties; and 7) severe OSA (Apnea–Hypopnea Index >30/h) in diagnostic HSAT. Eligible patients were clinically evaluated with the Consortium to Establish a Registry for Alzheimer's Disease Neuropsychological Battery (CERAD-NB) (21). To be applicable for the present imaging, they had to reach normal results in the CERAD-NB evaluation. In addition, APOE genotyping based on venous blood samples was performed.

The study has been approved by the institutional review board, and all subjects signed an informed consent form.

### *Structural imaging (MRI)*

A 3.0T MRI scanner (Philips Achieva TX 3T; Best, the Netherlands) and an 8-channel head coil were used for structural imaging. The protocol included 3D T1-weighted images (sagittal scan, 1.0 mm isotropic voxel), transaxial T2-weighted images (slice thickness of 3.0 mm, in-plane resolution of 0.45 mm x 0.45 mm), 3D fluid-attenuated inversion recovery (FLAIR) images (sagittal scan, 1.0 mm isotropic voxel), and susceptibility-weighted imaging (slice thickness of 1.0 mm, in-plane resolution of 0.45 mm x 0.45 mm). In addition, diffusion tensor imaging (DTI) was performed (slice thickness of 2mm, in-plane resolution 2.0 mm x 2.0 mm, diffusion directions: 16 unique directions at b0 = 800 s/mm$^2$ with 1 repetition at b0 = 0s/mm$^2$).

An experienced neuroradiologist evaluated all MR images for any WM abnormalities and the presence of microbleeds [for details, see Ylä-Herttuala et al. 2021 (3)].

### *MRI-based determination of regions of interest*

The high-resolution 3D T1-weighted images were used as reference images for PET. MRI-based structure templates and a multi-atlas segmentation algorithm (cNEURO software, Combinostics, Tampere, Finland) were used for PET and DTI region of interest (ROI) analyses (22, 23). The method for segmenting white matter hyperintensities from FLAIR images is described in (22).

### *Diffusion tensor imaging analysis*

Voxelwise statistical analysis of the DTI data was carried out using Tract-Based Spatial Statistics (TBSS) (24), part of the FSL software package (25). Fractional Anisotropy (FA) images were created by fitting a tensor model to the raw diffusion data using FDT from the FSL package. Using TBSS, all subjects' FA data were projected onto a mean FA tract skeleton before voxelwise cross-subject statistics was applied. In addition to FA images, the same analysis was performed to mean diffusion (MD), radial diffusion (RD), and axial diffusion (AD) images. One patient with decreased GM–WM contrast in [11C]-PiB uptake did not have DTI data, and one DTI dataset was excluded from the analysis because of large ventricles interfering with co-registration.

For ROI analysis, parametric DTI images were co-registered with the anatomical T1 images of each patient, and mean values for FA, MD, RD, and AD parameters were extracted using the above-mentioned ROIs.

### *Production of [11C]-PiB*

The radiotracer was produced following GMP protocol. All batches were controlled for chemical purity, chemical identity, radiochemical purity, radionuclide identity, pH, endotoxin levels, microbiological burden, solvent residuals, color, filter integrity, etc. to be suitable for use in human studies. The molecular activities were 110–190 GBq/umol and the radiochemical purity was over 99% (n = 19) in all patient doses used for this study.

### *Imaging of Aβ uptake with [11C]-PiB*

[11C]-PiB PET/computed tomography (CT) scans were performed using a Siemens Biograph mCT PET/CT

**Table 1.** The clinical and imaging characteristics of OSA patients with visually normal (n = 14) and abnormal (n = 5) contrast between the gray and white matter in [$^{11}$C]-PIB PET

| | Visually normal contrast | Visually abnormal contrast | p-value |
|---|---|---|---|
| Age (years) | 45.4 ± 5.6 | 41.0 ± 5.8 | NS |
| Sex (male %) | 71 | 80 | NS |
| APOE ε4 genotype e2/e3, e3/e3, e3/e4 (%) | 7, 64, 29 | 0, 100, 0 | NS |
| Smoking (%) | 14 | 80 | 0.007 |
| Body Mass Index (kg/m$^2$) | 35.9 ± 7.4 | 40.6 ± 13.3 | NS |
| Hypertension (%) | 36 | 60 | NS |
| Apnea–Hypopnea Index (events/hour) | 45.4 ± 11.0 | 79.0 ± 17.9 | 0.001 |
| CPAP therapy (%) | 86 | 60 | NS |
| Cerebral gray matter volume (ml) | 591 ± 47 | 556 ± 59 | NS |
| White matter hyperintensity volume (ml) | 0.6 ± 0.8 | 0.8 ± 0.5 | NS |
| Fractional anisotropy * | 0.41 ± 0.17 | 0.40 ± 0.15 | NS |
| Mean diffusion (x10$^{-3}$) * | 0. 79 ± 0.02 | 0. 81 ± 0.02 | NS |
| Gray matter SUV | 0.40 ± 0.09 | 0.36 ± 0.12 | NS |
| White matter SUV | 0.62 ± 0.14 | 0.43 ± 0.14 | 0.03 |
| Gray to white matter SUV ratio | 0.64 ± 0.03 | 0.85 ± 0.07 | <0.001 |

Values are mean ± standard deviation or percentage. * Diffusion tensor imaging analysis was available for 17 subjects (13 visually normal and 4 visually abnormal contrast). Abbreviations: CPAP = continuous positive airway pressure, SUV = standardized uptake value.

scanner (Siemens Healthcare, Erlangen, Germany). All 19 patients underwent a 30 min [$^{11}$C]-PiB static PET scan 60 min after intravenous injection of in-house-produced 550 MBq of [$^{11}$C]-PiB. In addition, 90 min [$^{11}$C]-PiB dynamic PET scans were performed for 10 patients starting at the moment of injection of the tracer. Static images were calculated from 60 to 90 min post injection for each patient. Dynamic acquisition included frames of 6 x 1 min, 6 x 2 min, 4 x 3 min, 6 x 5 min, and 3 x 10 min (total duration 90 min). CT scans were performed before PET imaging, and CT information was used for attenuation correction. All images were reconstructed on a 128 x 128 matrix using the ordered subsets expectation maximization iterative algorithm (4 iterations, 21 subsets, zoom 2, no post filter).

### *Analyses of PET-images*

All [$^{11}$C]-PiB images were first visually analyzed at the individual level. Two experienced nuclear medicine physicians visually graded patients based on radiotracer distribution in the brain. Subsequently, standardized uptake values (SUV) were determined for gray and white matter. In addition, the ratios of GM to WM uptake (standardized uptake value ratio, SUVR) were calculated. ROIs were delineated using patient-specific, T1-weighted MRI images using cNEURO software. All quantitative PET analyses were conducted using PMOD software (version 4.103, PMOD Technologies, Zürich, Switzerland). Retention indices were determined as a ratio of corresponding SUV at the post-injection time points of 1) maximum uptake value and maximum +9 min (~11 min), 2) 11 and 29 min, and 3) 29 and 90 min from dynamic PET data representing percentage change in SUV in early and late time points.

### *Statistical analysis*

The data were analyzed using tests for nonparametric distribution. Two groups were formed according to visual analysis of GM–WM uptake ratios in [$^{11}$C]-PIB PET (normal contrast, n = 14; decreased contrast, n = 5). For continuous variables, a comparison between the two groups was performed using the Mann–Whitney U test. A Chi-square test was applied to sets of categorical data. Univariate correlations were assessed using the Spearman correlation analysis. Selection of test variables in comparisons between the study groups and for univariate correlations was based on the most important clinical and imaging characteristics described in Tables 1 and 3. Statistical significance was indicated with the p-value <0.05. SPSS version 26 (SPSS Inc, Chicago, IL) was utilized to conduct statistical analysis.

## Results

### *Study sample and between-groups differences in demographic and clinical variables*

Globally decreased GM–WM contrast in PiB uptake was seen in 5 of the 19 patients. Based on this, the study population was divided into two groups: visually normal

**Table 2.** Retention indexes between different time points for OSA patients with visually normal (n = 7) and abnormal (n = 3) contrast between gray and white matter in [11C]-PIB PET. Max refers to time point of the highest standardized uptake value (SUV) or SUV ratio in radiotracer kinetics analysis

| | Visually normal contrast | Visually abnormal contrast | p-value |
|---|---|---|---|
| Gray matter | | | |
| Max to max +9 min | -37.1 ± 6.7 | -47.3 ± 3.1 | 0.033 |
| 11 to 29 min | -52.9 ± 2.9 | -53.0 ± 6.3 | NS |
| 29 to 90 min | -47.6 ± 3.8 | -16.1 ± 16.5 | 0.017 |
| White matter | | | |
| Max to max +9 min | -24.1 ± 5.8 | -34.8 ± 1.3 | 0.017 |
| 11 to 29 min | -31.8 ± 3.1 | -35.1 ± 4.7 | NS |
| 29 to 90 min | -38.4 ± 3.3 | -24.8 ± 11.2 | 0.017 |
| Gray / White matter | | | |
| Max to max +9 min | -19.2 ± 3.0 | -23.4 ± 1.4 | 0.033 |
| 11 to 29 min | -31.0 ± 1.7 | -27.8 ± 4.4 | NS |
| 29 to 90 min | -14.9 ± 5.3 | 11.1 ± 5.5 | 0.017 |

Values are mean ± standard deviation.

**Figure 1.** Illustrative examples of [11C]-PiB PET and T1-weighted MRI images of A) 49-year-old patient with typical normal visual appearance and B) 37-year-old patient with decreased gray–white matter tracer uptake contrast

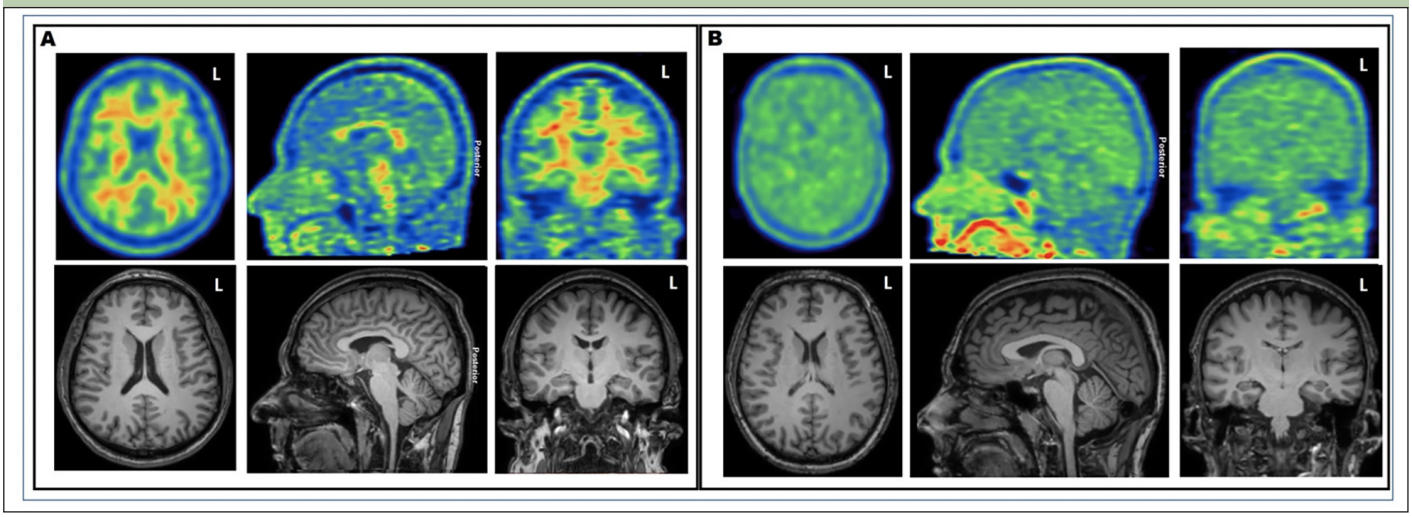


and visually abnormal contrast (table 1). There were statistically significant between-groups differences in smoking and AHI, whereas no statistical differences were seen in age, gender, BMI, hypertension, CPAP use, or APOE ε4 genotype.

## *Between-group neuroimaging comparisons*

A decrease in GM–WM contrast in PiB tracer uptake was seen at visual evaluation (see Fig. 1), and quantitative analyses further confirmed these findings (Fig.2). Dynamic PET imaging analyses revealed decreased GM–WM contrast in the later uptake phase (between 40 to 90 min after the injection), whereas at the initial phase (~ first 11 minutes after tracer injection), the GM and WM uptake was faster in patients with decreased GM–WM contrast than in those with normal GM–WM contrast (Table 2, Fig. 3).

Visual WM MRI analysis revealed small punctate foci in the deep WM (Fazekas Grade 1) in four patients, while the remaining 15 patients had no WM lesions or signs of microhemorrhages. There were no differences in DTI TBSS analyses between patient groups of normal and reduced GM–WM contrast in PiB uptake. Moreover, absolute quantitative WMH volumes were low in both groups and showed no difference between subjects with normal and abnormal GM–WM contrast (Tables 1 and 3).

## *The results of between-group correlation analyses*

The level of GM–WM contrast decrease was significantly associated with two clinical characteristics

(Tables 1 and 3, Fig. 4). A decrease in GM–WM contrast was statistically significantly associated with smoking and severity of OSA (higher AHI). On the other hand, age, gender, BMI, hypertension, CPAP use or APOE ε4 genotype status did not show similar associations. GM-WM SUV ratio showed significant difference between the groups (Tables 1 and 2).

**Figure 2.** [11C]-PiB PET gray/white matter standardized uptake value ratio (SUVR) in 1) visually normal and 2) abnormal uptake groups

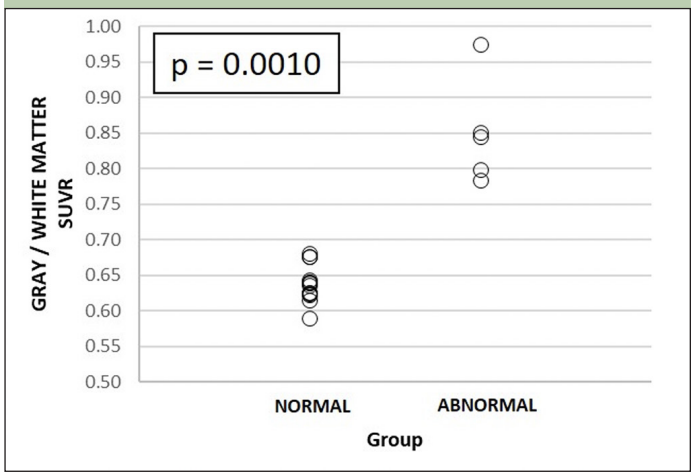


The p-value refers to statistically significant differences between groups 1 and 2, respectively.

**Table 3.** Univariate correlations of gray to white matter standardized uptake value ratio in [11C]-PiB with clinical and imaging characteristics

| | Spearman's rho | P-value |
|---|---|---|
| Age | -0.407 | 0.08 |
| Body mass index | -0.136 | 0.58 |
| Apnea hypopnea index | 0.539 | 0.017 |
| Cerebral gray matter volume | -0.16 | 0.513 |
| White matter hyperintensity volume | 0.295 | 0.22 |
| Fractional anisotropy | -0.115 | 0.66 |
| Mean diffusion | 0.029 | 0.91 |

## Discussion

We are not aware of previous studies of decreased GM–WM contrast in [11C]-PiB PET tracer uptake in cognitively intact, middle-aged subjects who displayed no or only minor structural WM changes in detailed MRI evaluation. This finding, obtained from patients with severe OSA, provides new evidence on the dynamics of altered amyloid metabolism and possibly subsequently developing cortical amyloid burden. GM–WM contrast of amyloid tracer uptake can thus be altered without coexisting underlying structural abnormalities. Importantly, the level of GM–WM contrast decrease correlated significantly with the main objective parameter of the severity of OSA, namely AHI. The patient´s age, gender, BMI, hypertension, CPAP use or APOE status did not show similar associations.

OSA may be considered a potential and modifiable (26, 27) target for AD prevention; for reviews, see, e.g., (28, 29, 30). OSA may even possibly initiate AD neuropathological processes (31). Recent studies have demonstrated higher amyloid burden (2) and increased cortical Aβ deposits (3) in middle-aged patients with severe OSA. Similar findings of amyloid deposits in AD-sensitive predilection areas have been also demonstrated in older, unimpaired subjects with OSA (1). These observations have shown cortical amyloid deposits, whereas no data on GM–WM contrast of PiB tracer uptake in OSA are available.

Conventionally, visual evaluation is based on changes in local GM-WM contrast. However, in the present study globally decreased GM-WM contrast was the most prominent abnormality. This gave rise to the idea of investigating whether it was explained by structural alterations in GM or in WM. The abnormality in GM-WM contrast was observed to occur equally in the whole area of the brain without localization to specific areas. Thus, instead of using the standard regional analysis, we decided to quantify the global GM-WM contrast and investigate if factors reflecting clinical and imaging characteristics are associated with it.

The mechanisms for decreased GM–WM contrast in PiB uptake are mostly unknown at the moment. Our dynamic data suggest that the initial radiotracer is introduced into the circulation in a similar manner, whereas tracer kinetics is faster during the first 10 minutes from maximum uptake in patients with decreased WM–GM contrast. Moreover, the later phase of the tracer clearance may be the time window of decreased WM–GM uptake contrast (see timescale in Fig. 3). This may indicate differences in tracer binding and clearance with these patients. Interestingly, dynamic PET-measured cerebrospinal fluid clearance has been suggested as a biomarker in AD and other neurodegenerative diseases (32).

The role of WM damage and Aβ burden has suggested possible common mechanisms in neurodegenerative and demyelinating diseases (33). Moreover, very recent MRI evidence in frontotemporal dementia and AD suggests that WM hyperintensities may occur in a process independent of and related to cortical atrophy (34). These mechanisms may also apply in relation to OSA entity. Several possible mechanisms have been suggested, such as OSA seems to impair WM integrity in vulnerable regions, in association with disease severity (7). In addition, cerebral abnormal myelin and axonal integrity has also been described in OSA (35). Recently, the severity of desaturations (i.e., hypoxia parameters) in OSA has been associated with decreased cortical thickness and WM integrity (36).

Our cohort showed normal DTI findings and small WML volumes. Thus, no structural WM changes that

**Figure 3.** [11C]-PiB dynamic time activity curves of gray matter (A and B), white matter (C and D), and SUVR (E, F) as a function of time for patients with normal (n = 7, blue line) and abnormal (n = 3, red line) visual uptake

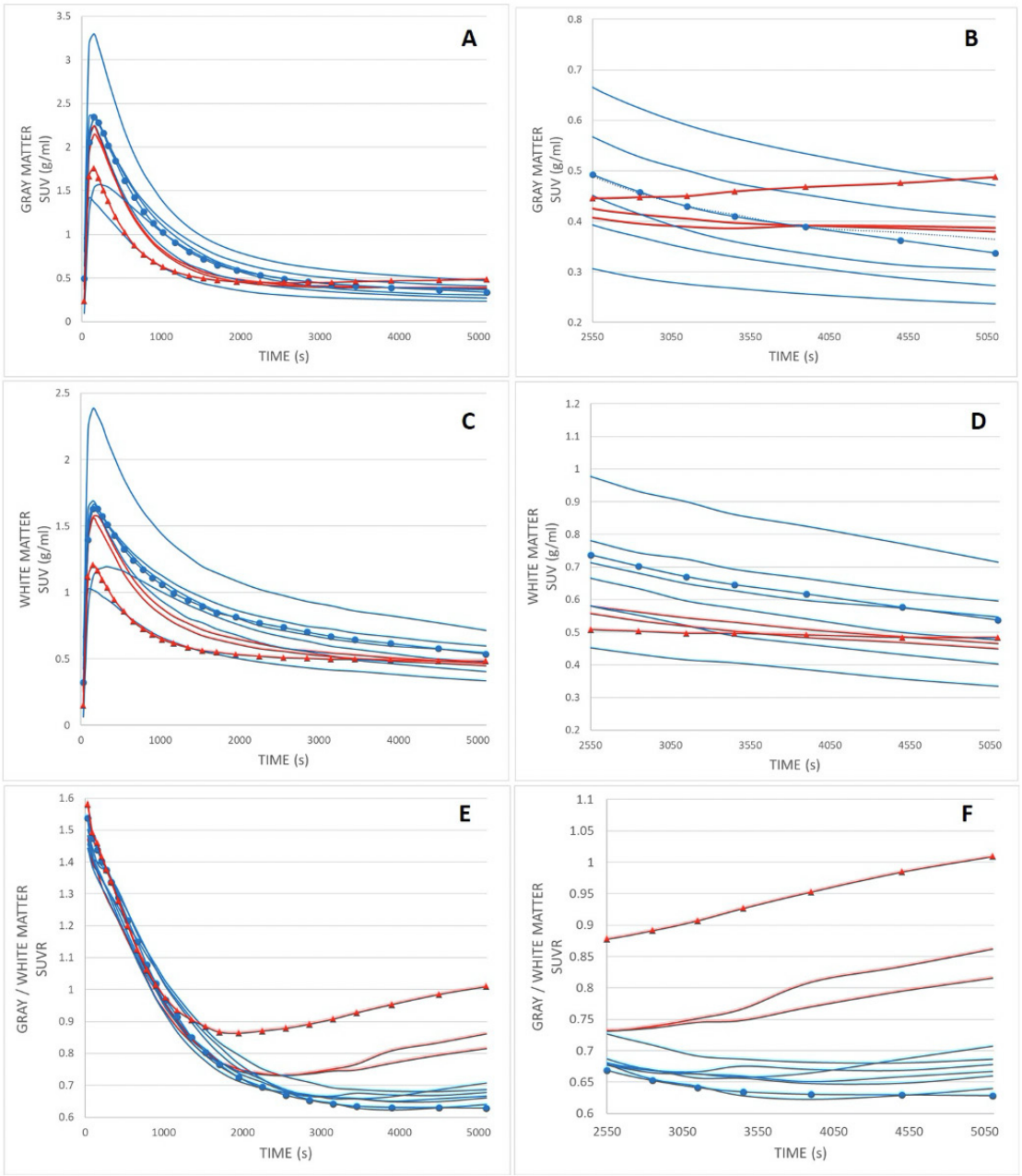


Retention indices were determined as a ratio of corresponding SUV values at post-injection time points of 1) maximum uptake value and maximum + 9 min (~11 min), 2) 11 and 29 min, and 3) 29 and 90 min for both groups, which are presented in Table 2. Symbols refer to corresponding patients with normal (circle) and decreased (triangle) gray–white matter uptake contrast, as presented in Figures 1A and B. Abbreviations: SUV = standardized uptake value, SUVR = standardized uptake value ratio.

could be attributable to altered GM–WM contrast of [11C]-PiB binding were seen. Recently, it has been suggested that the earliest accumulation of Aβ fibrils may occur before any structural alterations, leading initially to increased functional connectivity, and this increase may act as a compensatory mechanism to maintain cognitive functioning in spite of increased Aβ accumulation (19). Clinically, at least in severe OSA, frequent apneas and related abrupt arousals lead to highly disrupted sleep and numerous periods of nocturnal intermittent hypoxia. It is suggested that these core OSA symptoms may lead to, e.g., Aβ-metabolism dysregulation (31), and that disrupted sleep itself increases soluble amyloid (37). While sleep disruption in cognitively intact, elderly subjects is associated with brain imaging changes, it is still not fully understood whether it is the initial cause or represents structural or functional consequence; for a recent review, see (38).

Dynamic PET demonstrated that in some patients the amyloid PiB tracer uptake was eliminated/removed

more slowly than expected from GM and also WM. The biological background and possible behavioral consequences of the present findings are not clear at the moment. Our results demonstrate that GM–WM Aβ tracer kinetics itself may also be altered in severe OSA, resulting in decreased GM–WM uptake contrast. Amyloid [11C]-PiB imaging may visualize not only the amount and localization of amyloid depositions but also the dynamics of how tracer uptake is removed from GM and WM.

**Figure 4.** Correlation between gray to white matter ratio (SUVR) in [11C]-PiB PET and Apnea–Hypopnea Index

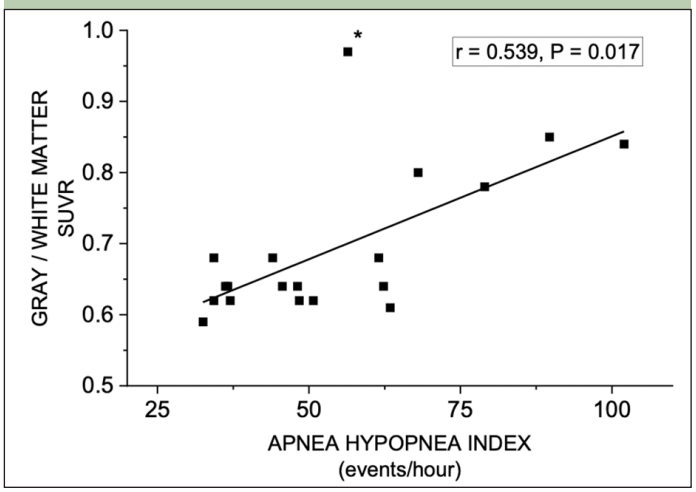


Note: "outlier" patient (*) had long apneas and hypopneas (46 s and 59 s, respectively), resulting in paradoxically lower value of AHI (56.4/h).

Cerebrospinal fluid plays an important role in solute clearance and maintenance of brain homeostasis. In addition, the glymphatic system has been suggested as being largely responsible for the clearance of waste from the brain. [11C]-PiB PET has been used to quantify cerebrospinal fluid clearance in humans. Our results may indicate that dynamic [11C]-PiB PET can be used to observe changes in [11C]-PiB retention and dynamics in OSA patients. The loss of GM–WM contrast indicates that [11C]-PiB retention may be altered unexpectedly in different diseases or disease stages, and this should be carefully considered when classical statistical [11C]-PiB analysis is carried out. Furthermore, our results provide new information for assessing [11C]-PiB brain clearance in OSA patients. We hope that this and future work in this area will improve understanding of the link between severe OSA and brain amyloid burden.

Clinically, our data with GM–WM contrast alterations further emphasizes and adds new evidence to the link between severe OSA and subsequent risk for AD. Importantly, these new findings are associated with the predisposing factor of smoking, and an objective parameter that reflects disease severity (AHI). On the other hand, age, sex, BMI, hypertension and the use of current treatment for OSA (CPAP) showed no statistically significant associations. The more severe the OSA, the more reduced the tracer uptake elimination is (based on correlation between AHI and decreased GM–WM contrast). The correlation between [11C]-PiB uptake and these two clinical variables is important and could reflect dysfunction of the brain glymphatic system, at least in severe in OSA. In particular, OSA is among the currently known disorders that impair the glymphatic system (39), and glymphatic failure has been proposed as a final common pathway to dementia (40).

## *Limitations*

The study is cross-sectional, and no follow-up data is yet available. One limitation is the lack of a control group. Our cohort was carefully selected to exclude possible factors that could alter GM–WM contrast. Within this carefully selected patient population, initial sub-group classification was based on normal clinical evaluation criteria in [11C]-PiB PET visual assessment. Based on visual evaluation, two groups were determined: patients with visually normal and abnormal findings. Patients with visually normal findings were considered as reference group - comparable to even normal healthy patients in terms of visual assessment, and those with abnormal findings were considered as an abnormal group. Future studies should include patients with moderate OSA or even matched controls without OSA. This would help to define whether similar changes seen here in severe OSA as decreased GM-WM contrast are evident with other clinical stages of OSA.

Our sample size was relatively small; however, it was comparable to recent similar studies, e.g., Jackson et al. (2). In addition, ethical issues may arise when including young, healthy control group because of radiation exposure. Finally, dynamic PET was not available for every subject.

## *Clinical significance*

Severe OSA was associated with previously undescribed decreased GM–WM contrast in amyloid tracer uptake, with significant correlation with the clinical parameters of smoking, and AHI. The study further supports the deleterious link between severe OSA and risk for AD. The decreased GM–WM ratio might reflect dynamic pathophysiological phenomena that occur prior to the change from normal GM–WM contrast to the appearance of cortical amyloid deposits in OSA.

*Funding:* This study was supported by grants from the Finnish Cultural Foundation and the Breathing Foundation of Kuopio Region, Finland. The sponsors had no role in the design and conduct of the study; in the collection, analysis, and interpretation of data; in the preparation of the manuscript; or in the review or approval of the manuscript. Open access funding provided by Kuopio University Hospital, University of Eastern Finland.

*Conflict of interest:* None of the authors have any financial or other substantial COI that might be construed to influence the results or interpretation of the manuscript. Salla Ylä-Herttuala: No conflict of interest; Mikko Hakulinen: No conflict of interest; Pekka Poutiainen: No conflict of interest; Jyrki Lötjönen: No conflict of interest; Mervi Könönen: No conflict of interest; Heidi Gröhn: No conflict of interest; Ritva Vanninen: No conflict of interest; Hanna Mussalo: No conflict of interest; Tomi Laitinen: No conflict of interest; Esa Mervaala: No conflict of interest.

*Ethical standards:* In all aspects of this research we followed the highest ethical standards, good scientific practice and respected human rights.



## References

1. André C, Rehel S, Kuhn E, et al. Association of sleep-disordered breathing with Alzheimer disease biomarkers in community-dwelling older adults: a secondary analysis of a randomized clinical trial. JAMA Neurol. 2020;77:716–724. https://doi.org/10.1001/jamaneurol.2020.0311.
2. Jackson ML, Cavuoto M, Schembri R, et al. Severe obstructive sleep apnea is associated with higher brain amyloid burden: a preliminary PET imaging study. J Alzheimers Dis. 2020;78:611. https://doi.org/10.3233/JAD-200571.
3. Ylä-Herttuala S, Hakulinen M, Poutiainen P, et al. Severe obstructive sleep apnea and increased cortical amyloid-β deposition. J Alzheimers Dis. 2021;79:153–161. https://doi.org/10.3233/JAD-200736.
4. Castronovo V, Scifo P, Castellano A, et al. White matter integrity in obstructive sleep apnea before and after treatment. Sleep. 2014;37:1465–1475. https://doi.org/10.5665/sleep.3994.
5. Zhang J, Weaver TE, Zhong Z, et al. White matter structural differences in OSA patients experiencing residual daytime sleepiness with high CPAP use: a non-gaussian diffusion MRI study. Sleep Med. 2019;53:51–59. https://doi.org/10.1016/j.sleep.2018.09.011.
6. Xiong Y, Zhou XJ, Nisi RA, et al. Brain white matter changes in CPAP-treated obstructive sleep apnea patients with residual sleepiness. J Magn Reson Imaging. 2016;45:1371. https://doi.org/10.1002/jmri.25463.
7. Chen H, Lu C, Lin H, et al. White matter damage and systemic inflammation in obstructive sleep apnea. Sleep. 2015;38:361. https://doi.org/10.5665/sleep.4490.
8. Lee M, Yun C, Min A, et al. Altered structural brain network resulting from white matter injury in obstructive sleep apnea. Sleep. 2019;42. https://doi.org/10.1093/sleep/zsz120.
9. Brown EE, Rashidi-Ranjbar N, Caravaggio F, et al. Brain amyloid PET tracer delivery is related to white matter integrity in patients with mild cognitive impairment. J Neuroimaging. 2019;29:721. https://doi.org/10.1111/jon.12646.
10. Zeydan B, Schwarz CG, Lowe VJ, et al. Investigation of white matter PiB uptake as a marker of white matter integrity. Ann Clin Transl Neurol. 2019;6:678–688. https://doi.org/10.1002/acn3.741.
11. Glodzik L, Rusinek H, Li J, et al. Reduced retention of Pittsburgh compound B in white matter lesions. Eur J Nucl Med Mol Imaging. 2015;42:97. https://doi.org/10.1007/s00259-014-2897-1.
12. Goodheart AE, Tamburo E, Minhas D, et al. Reduced binding of Pittsburgh compound-B in areas of white matter hyperintensities. Neuroimage: Clin. 2015;9:479–483. https://doi.org/10.1016/j.nicl.2015.09.009.
13. Wang Y, Hu H, Yang Y, et al. Regional amyloid accumulation and white matter integrity in cognitively normal individuals. J Alzheimers Dis. 2020;74:1261. https://doi.org/10.3233/JAD-191350.
14. Yi H, Won KS, Chang HW, Kim HW. Association between white matter lesions and cerebral Aβ burden. PLoS One. 2018;13:e0204313. https://doi.org/10.1371/journal.pone.0204313.
15. Kasahara H, Ikeda M, Nagashima K, et al. Deep white matter lesions are associated with early recognition of dementia in Alzheimer's disease. J Alzheimers Dis. 2019;68:797–808. https://doi.org/10.3233/JAD-180939.
16. Dupont PS, Bocti C, Joannette M, et al. Amyloid burden and white matter hyperintensities mediate age-related cognitive differences. Neurobiol aging. 2020;86:16–26. https://doi.org/10.1016/j.neurobiolaging.2019.08.025.
17. Chételat G, Murray M. Amyloid PET scan: staging beyond reading? Neurology. 2017;89:2029–2030. https://doi.org/10.1212/WNL.0000000000004678.
18. Grothe M, Barthel H, Sepulcre J, et al. In vivo staging of regional amyloid deposition. Neurology. 2017;89:2031–2038. https://doi.org/10.1212/WNL.0000000000004643.
19. Hahn A, Strandberg TO, Stomrud E, et al. Association between earliest amyloid uptake and functional connectivity in cognitively unimpaired elderly. Cereb Cortex. 2019;29:2173–2182. https://doi.org/10.1093/cercor/bhz020.
20. Berry RB, Budhiraja R, Gottlieb DJ, et al. Rules for scoring respiratory events in sleep: update of the 2007 AASM manual for the scoring of sleep and associated events. J Clin Sleep Med. 2012;8:597–619. https://doi.org/10.5664/jcsm.2172.
21. Morris JC, Heyman A, Mohs RC, et al. The consortium to establish a registry for Alzheimer's disease (CERAD). Part I. clinical and neuropsychological assessment of Alzheimer's disease. Neurology. 1989;39:1159-1165. https://doi.org/10.1212/wnl.39.9.1159.
22. Koikkalainen J, Rhodius-Meester H, Tolonen A, et al. Differential diagnosis of neurodegenerative diseases using structural MRI data. Neuroimage Clin. 2016;11:435–449. https://doi.org/10.1016/j.nicl.2016.02.019
23. Lötjonen JM, Wolz R, Koikkalainen JR, et al. Fast and robust multi-atlas segmentation of brain magnetic resonance images. Neuroimage. 2010;49:2352–2365. https://doi.org/10.1016/j.neuroimage.2009.10.026.
24. Smith SM, Jenkinson M, Johansen-Berg H, et al. Tract-based spatial statistics: voxelwise analysis of multi-subject diffusion data. Neuroimage (Orlando, Fla.). 2006;31:1487–1505. https://doi.org/10.1016/j.neuroimage.2006.02.024.
25. Smith SM, Jenkinson M, Woolrich MW, et al. Advances in functional and structural MR image analysis and implementation as FSL. NeuroImage. 2004;23:S208–S219. https://doi.org/10.1016/j.neuroimage.2004.07.051.
26. Liguori C, Mercuri NB, Izzi F, et al. Obstructive sleep apnea is associated with early but possibly modifiable Alzheimer's disease biomarkers changes. Sleep. 2017;40. https://doi.org/10.1093/sleep/zsx011.
27. Liguori C, Chiaravalloti A, Izzi F, et al. Sleep apnoeas may represent a reversible risk factor for amyloid-β pathology. Brain. 2017;140:e75. https://doi.org/10.1093/brain/awx281.
28. Andrade AG, Bubu OM, Varga AW, Osorio RS. The relationship between obstructive sleep apnea and Alzheimer's disease. J Alzheimers Dis. 2018;64:S255–S270. https://doi.org/10.3233/JAD-179936.
29. Baril A, Carrier J, Lafrenière A, et al. Biomarkers of dementia in obstructive sleep apnea. Sleep Med Rev. 2018;42:139–148. https://doi.org/ 10.1016/j.smrv.2018.08.001.
30. Polsek D, Gildeh N, Cash D, et al. Obstructive sleep apnoea and Alzheimer's disease: in search of shared pathomechanisms. Neurosci Biobehav Rev. 2018;86:142–149. https://doi.org/10.1016/j.neubiorev.2017.12.004.
31. Liguori C, Mercuri NB, Nuccetelli M, et al. Obstructive sleep apnea may induce orexinergic system and cerebral β-amyloid metabolism dysregulation: is it a further proof for Alzheimer's disease risk? Sleep Med. 2019;56:171–176. https://doi.org/10.1016/j.sleep.2019.01.003.
32. De Leon MJ, Li Y, Okamura N, et al. Cerebrospinal fluid clearance in Alzheimer disease measured with dynamic PET. J Nucl Med. 2017;58:1471. https://doi.org/10.2967/jnumed.116.187211.
33. Pietroboni AM, Colombi A, Carandini T, et al. The role of amyloid-β in white matter damage: possible common pathogenetic mechanisms in neurodegenerative and demyelinating diseases. J Alzheimers Dis. 2020;78:13. https://doi.org/10.3233/JAD-200868.
34. Huynh K, Piguet O, Kwok J, et al. Clinical and biological correlates of white matter hyperintensities in patients with behavioral-variant frontotemporal dementia and Alzheimer disease. Neurology. 2021;96:e1743–e1754. https://doi.org/10.1212/WNL.0000000000011638.
35. Kumar R, Pham TT, Macey PM, et al. Abnormal myelin and axonal integrity in recently diagnosed patients with obstructive sleep apnea. Sleep. 2014;37:723–732. https://doi.org/10.5665/sleep.3578.
36. Chokesuwattanaskul A, Chirakalwasan N, Jaimchariyatam N, et al. Associations between hypoxia parameters in obstructive sleep apnea and cognition, cortical thickness, and white matter integrity in middle-aged and older adults. Sleep Breath. 2021;25:1559–1570. https://doi.org/10.1007/s11325-020-02215-w.
37. Lucey BP, Hicks TJ, McLeland JS, et al. Effect of sleep on overnight cerebrospinal fluid amyloid β kinetics. Ann Neurol. 2018;83:197–204. https://doi.org/10.1002/ana.25117.
38. André C, Laniepce A, Chételat G, Rauchs G. Brain changes associated with sleep disruption in cognitively unimpaired older adults: a short review of neuroimaging studies. Ageing Res Rev. 2021;66:101252. https://doi.org/10.1016/j.arr.2020.101252.
39. Komaroff AL. Does sleep flush wastes from the brain? JAMA. 2021;325:2153–2155. https://doi.org/10.1001/jama.2021.5631.
40. Nedergaard M, Goldman SA. Glymphatic failure as a final common pathway to dementia. Science. 2020;370:50–56. https://doi.org/10.1126/science.abb8739.

How to cite this article: S. Ylä-Herttuala, M. Hakulinen, P. Poutiainen, et al. Decreased Gray–White Matter Contrast of [11C]-PiB Uptake in Cognitively Unimpaired Subjects with Severe Obstructive Sleep Apnea. J Prev Alz Dis 2022;3(9):499-506; http://dx.doi.org/10.14283/jpad.2022.24